Intracluster multiple trimeric cyclization of acrylonitrile clusters initiated by electron transfer from a potassium atom: Size-dependent pathways in metastable dissociation of K[s...

ARTICLE *in* THE JOURNAL OF CHEMICAL PHYSICS · SEPTEMBER 2002

Impact Factor: 2.95 · DOI: 10.1063/1.1500732

3 AUTHORS, INCLUDING:

Fuminori Misaizu
Tohoku University
83 PUBLICATIONS **1,564** CITATIONS

SEE PROFILE

Intracluster multiple trimeric cyclization of acrylonitrile clusters initiated by electron transfer from a potassium atom: Size-dependent pathways in metastable dissociation of $K^+(CH_2{=}CHCN)_n$ photoions

Keijiro Ohshimo, Fuminori Misaizu,[a] and Koichi Ohno
Department of Chemistry, Graduate School of Science, Tohoku University, Aramaki, Aoba-ku, Sendai 980-8578, Japan

(Received 7 March 2002; accepted 25 June 2002)

Size-dependent stabilities and intracluster reactions of potassium atom and acrylonitrile molecules (AN; $CH_2{=}CHCN$) clusters were investigated. Previously reported magic numbers (intensity anomalies) of $n=3k$ ($k=1-4$) using photoionization mass spectrum of $K(AN)_n$, and size-specific elimination reactions (HCN elimination from clusters of $n\geqslant 3$, and H_2 elimination from $n=3$ and 6 clusters) were explained by a cyclohexane derivative formation in an intracluster trimeric cyclization (anionic oligomerization) initiated by electron transfer from a K atom in $K(AN)_n$. To elucidate larger $K(AN)_n$ structures, unimolecular metastable dissociations of $K^+(AN)_n$ photoions were observed using a reflectron time-of-flight mass spectrometer. A metastable dissociation pathway of $n\rightarrow n-1$ (AN-loss) was predominantly observed for all parent sizes; furthermore, for parent ions with $n=6$, 9, and 12, pathway of $n\rightarrow n-3$ [$(AN)_3$-loss] was also observed. These size-dependent dissociation pathways of photoions are related to structures of neutral clusters since intramolecular bonds are expected to be formed in the oligomerization reactions in neutrals and to be conserved in the photoionization process. Parent clusters that cause the $n\rightarrow n-1$ dissociations have structures in which at least one AN monomer can coordinate without forming any chemical bonds. The observation of $n\rightarrow n-3$ pathways corresponds to the existence of isomers of $n=3k$ ($k=2-4$) clusters having k cyclohexane derivatives, which are formed by intracluster multiple trimeric cyclization reactions with $3k$ AN molecules in neutral clusters. The existence of at least two types of structural isomers (including reacted AN or unreacted AN) in these clusters is shown from these experimental results, and is further supported by calculations of the microcanonical dissociation rate constants for each pathway based on the Rice–Ramsperger–Kassel–Marcus theory. © *2002 American Institute of Physics.* [DOI: 10.1063/1.1500732]

I. INTRODUCTION

Successive bond-formation reactions of the constituent organic molecules in ionic clusters, known as intracluster ionic oligomerization (polymerization), have been extensively studied in the past decade due to their importance in practical applications. The main purpose of these studies was to understand, at microscopic levels, the geometrical configurations and dynamics during the early stages of these reactions in the condensed phase. There are two types of reaction mechanism in ionic polymerization: *cationic* polymerizations are initiated by an electron transfer from a vinyl molecule to an electron acceptor, whereas *anionic* polymerizations are initiated by an electron transfer to a vinyl molecule from an initiator (electron donor). Alkali metals, because of their low ionization energies, can act as effective initiators of anionic polymerization. Studies on intracluster ionic oligomerizations have been carried out on cluster cations and anions for cationic and anionic oligomerization reactions, respectively. Intracluster cationic oligomerization has been studied by several groups by using electron impact or photoionization techniques for the generation of cluster cations.[1–20] In the systematic studies by Garvey and co-workers, and El-Shall and co-workers, magic numbers (intensity anomalies) in mass spectra were found for cluster cations of several unsaturated organic molecules (such as isoprene, isobutene, acetylene, or propene), and it was shown that these magic numbers are related to the formation of cyclic compounds by intracluster cationic oligomerization.[2–6,14,20] In contrast, intracluster anionic oligomerizations have been studied by a relatively small number of groups.[21–30] Cluster anions of vinyl compounds that were produced by electron transfer using high-Rydberg rare gas atoms were investigated by Kondow and co-workers.[21–25] For cluster anions of acrylonitrile (AN; $CH_2{=}CHCN$), photodissociation, unimolecular, and collision-induced dissociations, and photoelectron spectrum were observed,[26–30] resulting in the observation of trimeric terminations for AN cluster anions. These studies confirmed that the intracluster oligomerization of a trimeric unit is initiated by an electron transfer to $(AN)_3$, forming a stable anion radical with a ring structure, which was assigned as 1,3,5-cyclohexanetricarbonitrile (CHTCN).

Previously, we carried out studies of intracluster anionic oligomerizations in *neutral* clusters.[31–33] In these studies, clusters of an alkali metal atom (M=Li, Na, and K) with

[a]Electronic mail: misaizu@qpcrkk.chem.tohoku.ac.jp

vinyl compounds (VC=AN, acrylic ester, methacrylate, and methyl vinyl ketone) were generated and detected using a photoionization time-of-flight mass spectrometer (TOF-MS). In these $M(VC)_n$ clusters, magic numbers of $n=3$ were routinely observed in the photoionization mass spectra. We found that the size-dependent stabilities of neutral clusters are reflected in the observed pattern of these mass spectra. Accordingly, the magic numbers were explained as the formation of cyclohexane derivatives resulting from the anionic oligomerization of a trimeric unit, initiated by an electron transfer from the alkali metal atom in neutral clusters. Magic numbers at $n=6$, 9, and 12 were also observed, along with $n=3$ in the photoionization mass spectra of $M(AN)_n$ (M=Na and K).[31,33] From the periodicity of the observed magic numbers, formation of plural CHTCNs were expected. However, definitive evidence of the structures of larger clusters have been difficult to obtain using solely mass spectra data.

It has been reported that by using the fragmentation patterns in unimolecular metastable dissociation of size-selected cluster cations, information on the structure of clusters can be obtained.[18,34–40] For example, in the case of carbon clusters,[35] a neutral C_3-loss was mainly observed below C_{30}^+, whereas a C_2-loss was the dominant channel above C_{30}^+. These results were interpreted in terms of the stable structures of both the parent ions and the neutral fragments, which have been predicted theoretically. Intracluster oligomerization reactions of alkene cluster ions have also been investigated by the observation of metastable dissociations.[18] A recent study on multiphoton-ionized thymine cluster ions showed that, in metastable dissociations, parent ions consisting of an even number of molecules tend to lose two molecules, whereas those consisting of an odd number of molecules lose one molecule.[39] It was concluded that the two-molecule loss is a single fission process of a dimeric unit that is formed by intracluster photodimerization of thymine in the multiple absorption process.

Herein we report our investigations on the clusters of a K atom with AN molecules, $K(AN)_n$, by photoionization mass spectrometry using a reflectron TOF-MS. Similar to the previous study, the magic numbers from the mass spectra were observed at $n=3k$ ($k=1$–4).[31,33] In addition, size-specific elimination reactions were observed for $K(AN)_n$. Discussions are presented for these observations in relation to the formation of cyclohexane derivative by intracluster anionic oligomerization (trimeric cyclization) initiated by electron transfer from the K atom in $K(AN)_n$. Metastable dissociation reactions of $K^+(AN)_n$ photoions were also closely examined to elucidate the structures of large $K(AN)_n$ clusters. The oligomerized constituents in neutral clusters remain in photoions. Specifically, due to the small excess energy caused by one-photon ionizations, dissociation reactions of intramolecular bonds in clusters hardly occur following photoionization. The observed fragmentation pathways are relatively simple due to the small excess energy, where the metastable dissociations corresponding to the loss of a single AN molecule were exhibited for all parent cluster ions, and additionally, the loss of an $(AN)_3$ group from the parent cluster ion was observed for $n=6$, 9, and 12. Using these size-dependent fragmentation patterns, the stabilities and structures of $K^+(AN)_n$ photoions and the existence of structural isomers are discussed. Possible parent ion structures are also examined from calculations of the microcanonical rate constants for unimolecular dissociations based on the Rice–Ramsperger–Kassel–Marcus (RRKM) theory.

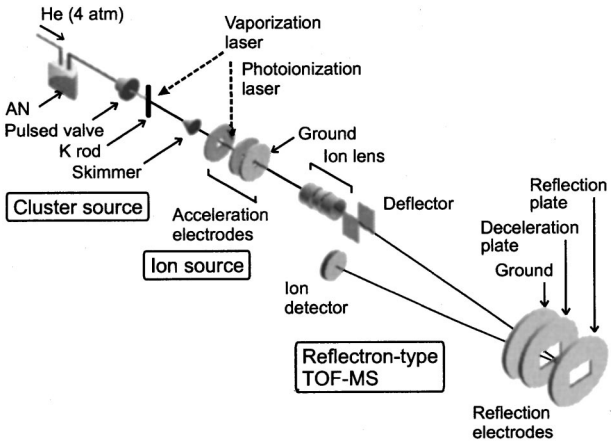

FIG. 1. Schematic diagram of the experimental setup.

II. EXPERIMENTAL SETUP

Present experiments were performed by using an apparatus composed of three-stage differentially evacuated chambers: a cluster source, an ion source by photoionization, and a home-made angular type reflectron TOF-MS. Schematic diagram of the experimental setup is shown in Fig. 1. Pressures of the chambers of cluster source, ion source, and reflectron were maintained at about 2×10^{-5}, 2×10^{-7}, and 8×10^{-8} Torr during measurements, respectively. Clusters of a K atom and AN molecules, $K(AN)_n$, were produced by a pickup source[31–33,41,42] with a combination of laser vaporization and pulsed supersonic expansion. After collimation with a conical skimmer, the neutral clusters were ionized by irradiation with a pulsed laser beam in a source region of the TOF-MS at 190 mm downstream from the pulsed valve (General Valve, series 9, orifice diameter 0.8 mm). A frequency-doubled output of a dye laser (Spectra-Physics, PDL-2 and Inrad, Autotracker III) pumped by a Nd:YAG laser (Spectra-Physics, GCR-150-10) was used as a photoionization light source. To avoid multiphoton processes, fluence of the ionization laser was kept $\lesssim$0.2 W/cm^2 throughout the measurements. By measuring the ionizing laser power dependence of cluster ion intensities, we confirmed that photoionization is a one-photon process. Product photoions were accelerated to $eU_0=+3085$ eV by static electric fields between acceleration electrodes. After traveling a field-free drift region between grounded plates of acceleration and reflection electrodes, these ions were reflected back to an ion detector by reflection electrodes. Two electric fields (decelerating and reflecting regions) were made by three plates (grounded, deceleration, and reflection plates) of reflection electrodes. Detection of cluster ions was carried out with a dual microchannel plate (MCP, Hamamatsu Photonics, F1552-21S). Mass resolution of the present reflectron TOF-MS is about 950. In measurements of ionization thresh-

old (I_{th}) of clusters, each photoion yield was measured with scanning the photon energy of the ionization laser, while abundance of clusters was alternately monitored by photoionization with fourth harmonic of another Nd:YAG laser (Lumonics, HY-400, 4.66 eV, 266 nm). The I_{th} values of the clusters were determined from the final decline of the photoionization efficiency (PIE) curves.

Along with the above measurements, mass spectra of $K^+(AN)_n$ ions nascently formed in the cluster source were also measured. Cluster ions were generated by an ion–molecule (cluster) reaction between a K^+ ion made by laser vaporization and neutral AN clusters in the expansion region of the free jet. These cations were introduced to the acceleration region of TOF-MS and were accelerated to $eU_0 \sim +1150$ eV by pulsed electric fields generated by high voltage pulse generators (DEI, GRX-1.5K-E). The timing of the acceleration field pulse with respect to the others was optimized by a digital delay/pulse generator (Stanford Research System, DG535).

In metastable dissociation reaction of $K^+(AN)_n$ clusters,

$$K^+(AN)_n \rightarrow K^+(AN)_m + (AN)_{n-m} \quad (1)$$

in the field-free drift region before reflection electrodes of the reflectron TOF-MS, the daughter ions, $K^+(AN)_m$, have an averaged laboratory-frame kinetic energies,

$$E_d = \frac{m_d}{m_p} eU_0, \quad (2)$$

where m_d and m_p are the mass of the daughter and the parent ions, respectively. Therefore, by setting a voltage of reflection plate (U_k) in the range between $(m_d/m_p)U_0$ and U_0, only the daughter ions are reflected back to the MCP detector. From the ionization laser power dependence, present dissociation process is confirmed to be not due to the photon absorption after photoionization. Collision-induced dissociation process of cluster ions can also be neglected under low pressure condition of the drift region ($\sim 8\times10^{-8}$ Torr) in the present experiment.

III. PHOTOIONIZATION MASS SPECTRUM OF K(AN)$_n$

A. Magic numbers in the photoionization mass spectrum

Figure 2(a) shows a typical mass spectrum of $K(AN)_n$ clusters obtained by one-photon ionization with a laser beam of 5.64 eV (220 nm). A series of $K^+(AN)_n$ cluster ions was predominantly observed up to $n=20$. Ion intensities of $n=3$, 6, and 9 were strongly observed with respect to adjacent n ions, and an intensity gap between $n=12$ and 13 was also observed. These magic numbers at $n=3k$ ($k=1$–4) in $K^+(AN)_n$ were also observed in mass spectra of $M(AN)_n$ (M=Na and K) in a previous study using a linear Wiley–McLaren type TOF-MS.[31,33] This magic-number behavior was independent of the photon energy of the ionization laser in the region between 4.66 and 5.64 eV.[33] This behavior was also independent of condition of the cluster source (intensity of the vaporization laser, stagnation pressure, and so on). We have also measured a mass spectrum of $K^+(AN)_n$ ions nascently formed by an ion-molecule reaction in the cluster source as shown in Fig. 2(b). Size distribution in this mass spectrum is expected to depend on stabilities of ions. As shown in the figure, a series of cluster ions of $K^+(AN)_n$ was observed up to $n=20$. Ion intensities decreased monotonically with increasing n, and the magic-number behavior at $n=3k$ in Fig. 2(a) was not observed in this mass spectrum. Therefore, we can assume that the stabilities of $K^+(AN)_n$ ions formed in the source does not depend sensitively on n, and that the magic numbers are related to the nature of neutral $K(AN)_n$ clusters.

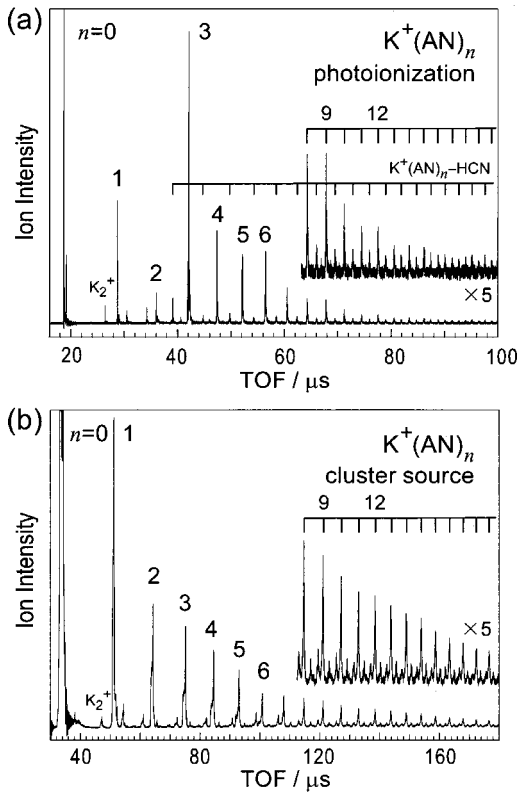

FIG. 2. (a) Photoionization mass spectrum of $K(AN)_n$ obtained by one-photon ionization of 5.64 eV. The number n in the figure represents the $K^+(AN)_n$ ion. The acceleration and reflector voltages are $U_0=+3085$ and $U_k=+3300$ V, respectively. $K^+(AN)_n$–HCN indicates ions with the loss of HCN from $K^+(AN)_n$ ions. (b) The mass spectrum of $K^+(AN)_n$ ions produced by ion–molecule reaction in the cluster source ($U_0 \sim +1150$ V, $U_k=+1220$ V).

Ionization thresholds (I_{th}) of $K(AN)_n$ ($n \leqslant 6$) were determined from measurements of PIE curves for these clusters as shown in Fig. 3. The I_{th} values are summarized in Table I: for $n=1$ I_{th} was determined to be 3.48 eV, and for $2 \leqslant n \leqslant 6$ the values were 3.53–3.61 eV. In our previous study,[31] the I_{th} values of $Na(AN)_n$ ($2 \leqslant n \leqslant 6$) were found to be constant at 3.63 ± 0.14 eV. These low I_{th} values correspond to low ionization energies of alkali metal atoms, 5.14 eV for Na and 4.34 eV for K.

The following factors causing magic numbers in photoionization mass spectra were already discussed in the previous papers:[31,33] (1) size-dependent stability of neutral clusters, (2) ionization cross sections of neutral clusters at certain photon energy for ionization, and (3) evaporation process after ionization. Among these, we can assume that the ionization cross section [possibility (2)] is not sensitively depen-

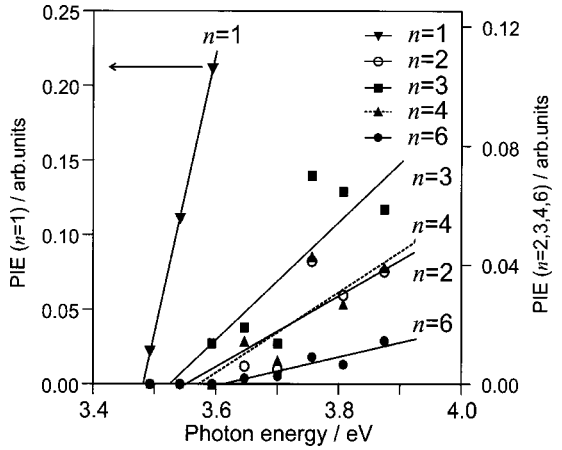

FIG. 3. Photoionization efficiency (PIE) curves for $K(AN)_n$ (n=1, 2, 3, 4, and 6). Left axis represents PIE values of n=1, and right axis represents those of the other clusters. These data are fitted with straight lines obtained by least-squares method. The dotted line is used for n=4, and solid lines are used for the others.

dent on n for all clusters in the present mass spectrum, because the photon energy is much higher than I_{th} of $K(AN)_n$ clusters for $2 \leqslant n \leqslant 6$ (3.53–3.61 eV). In addition, in the photoionization mass spectra even at the photon energy below 4.0 eV, the ion peak of n=3 was observed more intensely than those of n=2 and 4, as depicted in Fig. 3. Because we confirmed that the present photoionization is a one-photon process as noted in Sec. II, excess energy deposited in the photoion is less than the difference between the photon energy and I_{th}. With the photon energy below 4.0 eV, the excess energy is too small to induce evaporation processes after photoionization (metastable dissociation). Therefore, the appearance of the magic number is little affected by evaporation process after photoionization [possibility (3)]. After all, the magic numbers at $n=3k$ observed in the photoionization mass spectrum of $K(AN)_n$ are concluded to be due to the relative stabilities of neutral clusters [possibility (1)]. Furthermore, photodissociation experiment of neutral $K(AN)_n$ clusters revealed that the photoion intensity at n=3 is enhanced after photodissociation.[33] This result also indicates that the *neutral* $K(AN)_3$ has an anomalous stability relative to other sizes of clusters.

Cluster anions of AN that were produced by electron transfer using high-Rydberg rare gas atoms were extensively investigated by Kondow and co-workers. In the studies of mass spectrometry of $(AN)_n^-$,[21,25] magic numbers at $n=3k$ (k=1–3) were observed. They concluded that intracluster trimeric cyclization is initiated by an electron transfer to $(AN)_3$ forming a stable anion radical with a ring structure, which was assigned as 1,3,5-cyclohexanetricarbonitrile (CHTCN).[21,25–28,30] This trimeric cyclization is regarded as one of processes of anionic polymerization, which is known in condensed phase. Therefore, observed magic numbers at n=3 in $K(AN)_n$ are also due to the formation of CHTCN by intracluster trimeric cyclization initiated by an electron transfer from a K atom shown in Fig. 4, as concluded in the previous papers.[31,33]

TABLE I. Determined ionization thresholds (I_{th}) of $K(AN)_n$ clusters.

n	I_{th}/eV
0	4.34[a]
1	3.48
2	3.55
3	3.53
4	3.57
5	3.55
6	3.61

[a]Reference 53.

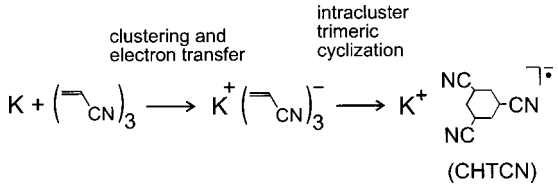

FIG. 4. Reaction scheme of the intracluster trimeric cyclization of $(AN)_3$ initiated by electron transfer from a K atom.

B. Size-specific elimination reactions of neutral $K(AN)_n$ clusters induced by cyclization reaction

In Fig. 2(a), fragment ions with a loss of HCN from $K^+(AN)_n$ were observed for $n \geqslant 3$ along with the series of $K^+(AN)_n$ clusters. Enlarged mass spectra of Fig. 2(a) are shown in Fig. 5. In n=3 and 6, ions with a loss of H_2 from

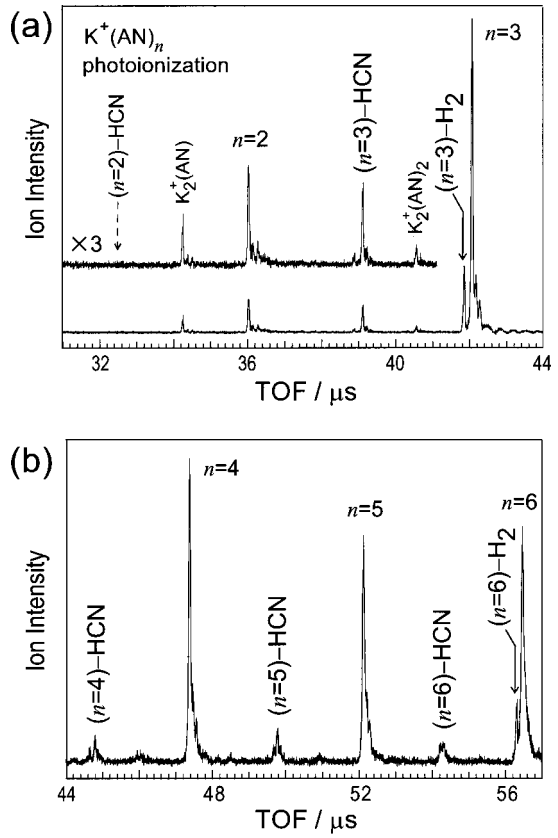

FIG. 5. Photoionization mass spectrum of $K(AN)_n$ obtained by one-photon ionization of 5.64 eV [(a) n=2, 3; (b) n=4–6]. The ordinate of (b) is scaled up by a factor of 3 from that of (a). Ions with elimination of H_2 and HCN are denoted by $-H_2$ and –HCN, respectively.

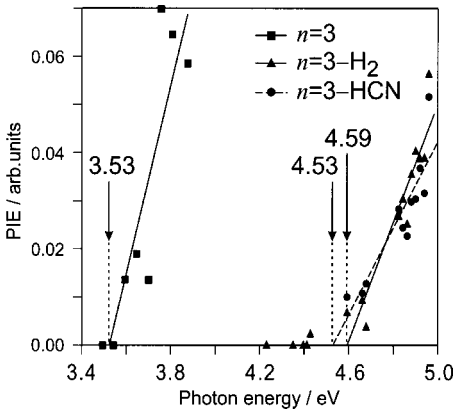

FIG. 6. Photoionization efficiency (PIE) curves for $K(AN)_3-H_2$ and $K(AN)_3-HCN$ along that for $K(AN)_3$.

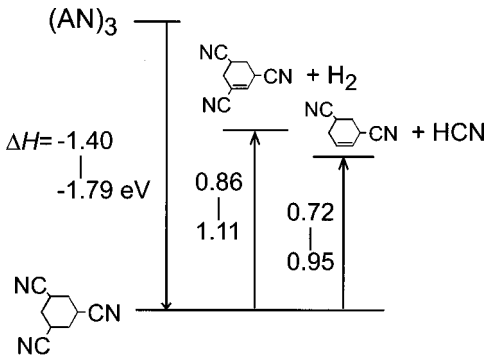

FIG. 7. Schematic energy diagram of the heat of reaction (ΔH) forming CHTCN from $(AN)_3$ and elimination reactions of H_2 and HCN from CHTCN. Total energy of a CHTCN (E[CHTCN]) and that of an $(AN)_3$ cluster ($E[(AN)_3]$) were used for estimation of ΔH for the formation of CHTCN ($\Delta H = E$[CHTCN]$-E[(AN)_3]$). In the estimation of heat of reaction for elimination of H_2 or HCN from CHTCN, E[CHTCN] and total energies of $C_9H_7N_3$, $C_8H_8N_2$, H_2, and HCN were used. These total energies were calculated by quantum chemical calculations using B3LYP/6-31+G* level with zero-point vibrational energy corrections. The ΔH values are not single value because CHTCN has four different isomers owing to axial-equatorial conformation of CN groups.

$K^+(AN)_n$ were also observed along with the series of $K^+(AN)_n$ and $K^+(AN)_n-HCN$.[43] On the other hand, no elimination reaction from $n=2$ was observed. If excitation of an AN molecule by absorption of the vaporization laser leads to the observed elimination reactions, these eliminations will be observed for all cluster sizes. Therefore, these size-specific elimination reactions are thought to be independent of the vaporization laser. In our previous studies of photoionization mass spectra of $M(AN)_n$ (M=Na and K) using Wiley-McLaren type TOF-MS,[31,33] these elimination reactions were difficult to be assigned because of its low mass resolution.

We have determined appearance energies of $K^+(AN)_3-H_2$ and $K^+(AN)_3-HCN$ by measuring the ion intensities with scanning the photon energy of the ionization laser. Observed PIE curves for these clusters are shown in Fig. 6 along with that for $K(AN)_3$. The appearance energies were found to be 4.53 and 4.59 eV for $K^+(AN)_3-H_2$ and $K^+(AN)_3-HCN$, respectively. If elimination reactions proceed in unreacted solvation-type clusters, eliminations are expected to be induced by excess energy caused by photoionization. Because the I_{th} of $K(AN)_3$ was found to be 3.53 eV, the minimum energy which is needed to induce elimination reactions will be ~1.0 eV. However, in recent high level *ab initio* calculations on AN (QCISD(T)/6-311++G(*d*,*p*)), the HCN or H_2 elimination reaction from an AN molecule ($CH_2{=}CHCN \rightarrow HCN + C_2H_2$ or $CH_2{=}CHCN \rightarrow H_2 + HC{\equiv}CCN$) was found to be endothermic by 1.68 and 1.81 eV, respectively.[44] Therefore, these elimination reactions do not proceed in the photoionization of solvationlike clusters.

As noted in the previous section, the intracluster cyclization reaction is found to proceed in $K(AN)_n$ ($n \geq 3$) clusters. Therefore, next we consider energetics of elimination reactions from CHTCN in reacted clusters. We have estimated heat of reaction (ΔH) forming CHTCN by theoretical calculations using GAUSSIAN 94.[45] Total energies were calculated on the basis of density functional theory (B3LYP/6-31+G*) for structures optimized by HF/6-31+G* level. The total energy of CHTCN (E[CHTCN]) and that of AN trimer ($E[(AN)_3]$) were used for estimation of ΔH. Because a CHTCN molecule is formed by the intracluster cyclization of AN trimer, ΔH can be estimated by using an equation, $\Delta H = E$[CHTCN]$-E(AN)_3$]. Vibrational frequencies calculated by HF/6-31+G* level were scaled to perform zero-point vibrational energy corrections. A scaling factor of 0.877 was used in the corrections, which was obtained from an average ratio of experimental[46] and calculated frequencies of normal modes in AN. For simplicity, the K atom was omitted in these calculations. The intracluster trimeric cyclization forming CHTCN was found to be exothermic by 1.40–1.79 eV. Energy uncertainty of 0.39 eV is due to four conformational isomers of CHTCN in which each of three substituents (–CN) forms an axial or an equatorial conformation. We have also estimated energies necessary for H_2 or HCN elimination from CHTCN using the same method. These reactions were found to be endothermic by 0.86–1.11 eV for the H_2 loss and 0.72–0.95 eV for the HCN loss. The calculated results on the energetics, summarized in Fig. 7, show that the elimination reactions can be induced by the excess energy generated by formation of CHTCN (ΔH). This is consistent with the experimental result shown in Fig. 5 in which no elimination reaction is observed from $n=2$, because no cyclization reaction takes place in $K(AN)_2$ due to the large ring strain. If we assume that elimination reactions proceed in photoions containing CHTCN, the minimum energy needed to induce the reactions is estimated to be 1.0 eV from the measurements of appearance energies, as noted above. This value is about 0–0.3 eV larger than those necessary for H_2, HCN elimination. However, a reaction barrier of each elimination reaction is considered to be much higher than 1.0 eV. Therefore, these elimination reactions are expected to hardly proceed in the photoions. In the mass spectrometric studies of cluster anions of AN,[21,25] the H_2 and HCN elimination reactions were also observed in $(AN)_n^-$ for $n=3$, 6 and $n \geq 3$, respectively. In their studies, it was also concluded that these elimination reactions are induced by the excess energy generated by the intracluster trimeric cyclization of $(AN)_3^-$ to form $CHTCN^-$. In the present $K(AN)_n$ clusters, the same

reason can be applicable to explain these elimination reactions.

In Fig. 5, the H_2 elimination reaction was observed only from $n=3$ and 6, while the HCN elimination was observed from the clusters of $n \geqslant 3$. It is worth noting about these size-specific elimination reactions. In the HCN elimination reaction, height of the reaction barrier against the total energy of CHTCN is considered to be lower than the value of ΔH, because this elimination was observed in all sizes of $n \geqslant 3$. In the H_2 elimination, the reaction barrier is presumed to be higher than ΔH except for $n=3$ and 6. The reason of this size dependence of the height of reaction barrier is unclear at present. However, it may be due to a difference in geometrical structures of these clusters. As discussed in Sec. III A and in our previous papers,[31,33] one and two CHTCN(s) are expected to be formed by intracluster cyclization(s) in $K(AN)_3$ and $K(AN)_6$, respectively. It is also confirmed that these structural isomers with no unreacted AN monomer exist for $n=3$ and 6 from observation of metastable dissociation of photoions as discussed in Sec. IV. On the other hand, all of the clusters with other sizes ($n \neq 3k$) contain at least one unreacted AN molecules. This difference of structures is probably related to the H_2 elimination reaction.

IV. METASTABLE DISSOCIATION OF $K^+(AN)_n$ PHOTOIONS

A. Size-dependent pathways in metastable dissociation of photoions

Figure 8(a) shows typical mass spectra obtained by one-photon ionization of $K(AN)_n$ by irradiation with 5.64 eV photon. From Figs. 8(a)(i) to 8(a)(iii), the voltage of reflection plate (U_k) was decreased from +3100 to +3060 V with the ion acceleration voltage (U_0) fixed at +3085 V. In Fig. 8(a)(i), small peaks indicated by circles were observed adjacent to peaks of the parent $K^+(AN)_n$ ions. With decreasing U_k from +3100 to +3080 V [Fig. 8(a)(ii)], the intensities of these small peaks were almost unchanged while those of parent ions decrease. At $U_k=+3060$ V [Fig. 8(a)(iii)], only the ion peaks denoted by the circles were observed, while the parent $K^+(AN)_n$ ions were no longer reflected back to the detector. Therefore, these ions observed in Fig. 8(a)(iii) are assignable to daughter ions caused by unimolecular metastable dissociation in the first field-free drift region. In general, two kinds of daughter ion signals are found in observation of metastable dissociation using reflectron TOF-MS; sharp ion peaks are due to daughter ions caused by metastable dissociation in the first drift region, and peaks appeared at a shoulder of large TOF side of parent ions are assignable to daughter ions produced in the acceleration region of TOF-MS.[47] In an enlarged figure of Fig. 8(a)(iii) [Fig. 8(b)], the series of daughter ions caused by metastable dissociation in the drift region were observed. By calculating TOF of these daughter ions, the observed peaks were assigned to daughter ions formed by metastable dissociation reactions, $K^+(AN)_n \rightarrow K^+(AN)_m + (AN)_{n-m}$, which is designated by $n \rightarrow m$. In addition, peaks with asterisks in Fig. 8(b) were assignable to $K^+(AN)_6$ and $K^+(AN)_7$ daughter ions caused by fast metastable dissociation in the acceleration region. For larger clusters, the daughter ions caused by fast dissociation were also observed as shown in Fig. 8(a)(iii). Following the discussion in this section, we concentrate on the daughter ions caused by metastable dissociation in the first drift region.

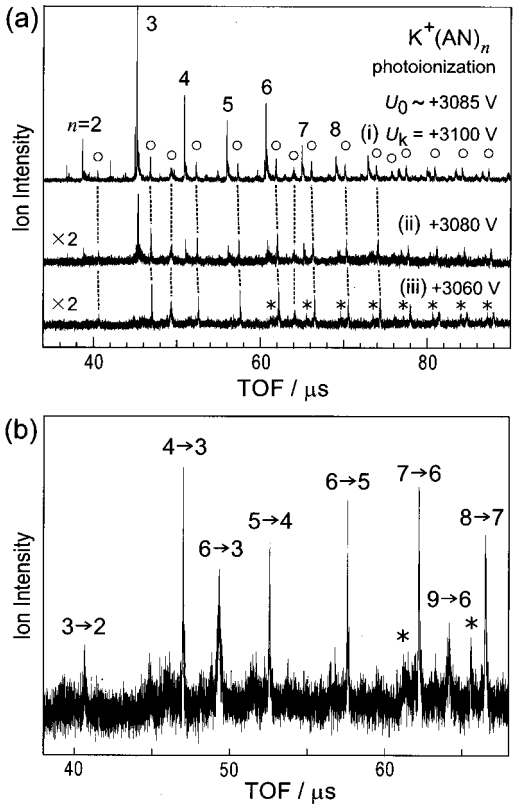

FIG. 8. (a) Photoionization mass spectra of $K(AN)_n$ obtained by one-photon ionization of 5.64 eV. These spectra are measured as a function of the reflector voltage (U_k) with a fixed acceleration voltage $U_0=+3085$ V: (i) $U_k=+3100$ V, (ii) +3080 V, and (iii) +3060 V. The number n in the figure represents parent $K^+(AN)_n$ ions. Peaks denoted by circles are assigned to the daughter ions caused by metastable dissociation in the first field-free drift region of reflectron TOF-MS. Peaks denoted by asterisks are assignable to the daughter ions caused by fast metastable dissociation in the acceleration region of TOF-MS. (b) Enlarged figure of the mass spectrum (a-iii). The $n \rightarrow m$ indicates the daughter ions formed by metastable dissociation, $K^+(AN)_n \rightarrow K^+(AN)_m + (AN)_{n-m}$, in the first field-free drift region. Peaks denoted by asterisks are $K^+(AN)_6$ and $K^+(AN)_7$ daughter ions caused by fast metastable dissociation in the acceleration region of reflectron TOF-MS.

In the present experimental condition, excess energy in a parent photoion was relatively small because photoionization was confirmed to be a one-photon process. Therefore, multiple metastable dissociation processes hardly occur from $K^+(AN)_n$ photoions. Also in previous studies of metastable dissociation following photoionization of atomic and molecular clusters, a loss of single molecule from a parent ion was observed as a dominant dissociation pathway, and multiple evaporation processes of more than one molecule were hardly observed.[38,48–52] As shown in Fig. 8(b), a metastable dissociation pathway of $n \rightarrow n-1$ (AN-loss) was observed for all parent sizes. In addition, daughter ions caused by a pathway of $n \rightarrow n-3$ were also observed only from the parent ions of $n=6$ and 9. Because the observed metastable dissociation was a single process, this pathway is described as $(AN)_3$-loss rather than 3(AN)-loss. Observed linewidths of

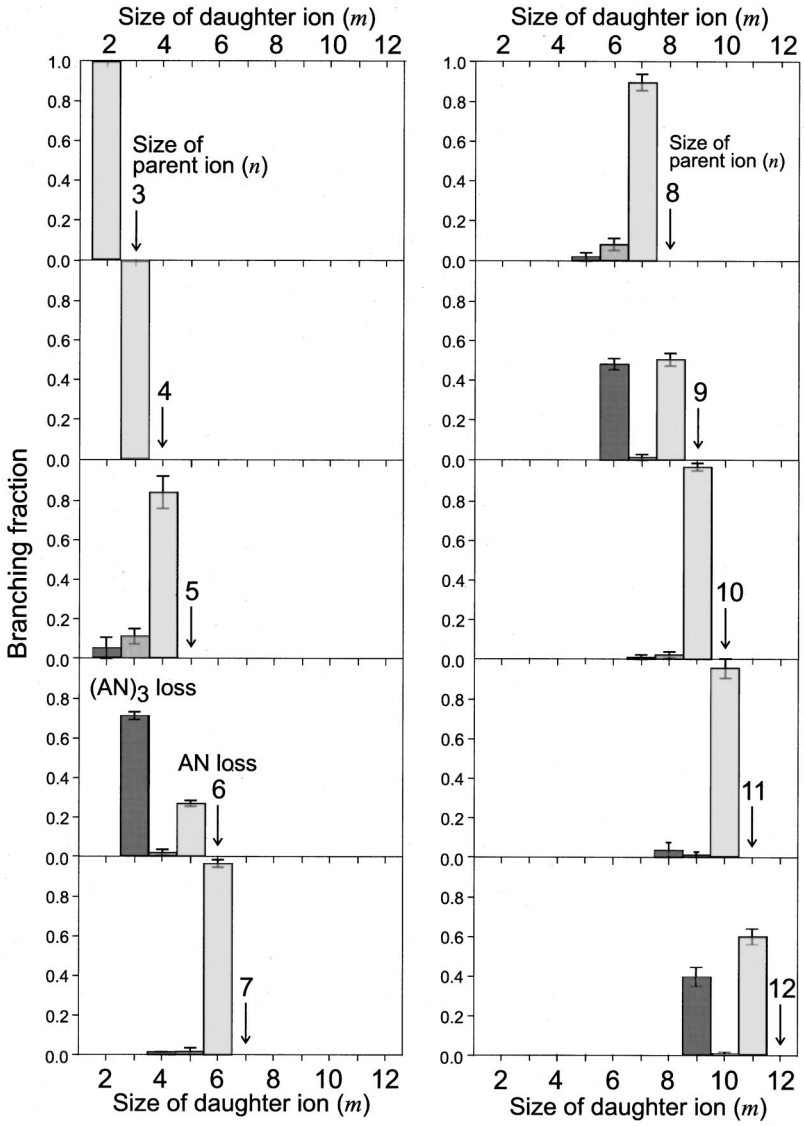

FIG. 9. Fractional size distribution of daughter ions, $K^+(AN)_m$, produced by metastable dissociation of each parent ion, $K^+(AN)_n$ (n=3–12). An arrow in each figure indicates the size of parent ions.

metastable dissociation peaks of 6→3 and 9→6 pathways were larger than those of $n \rightarrow n-1$ pathways. This is due to the difference of energy focusing effect in the reflection electrodes for daughter ions and is not due to dissociation dynamics. From Eq. (2), the daughter ions caused by the $n \rightarrow n-3$ dissociation has smaller kinetic energy (E_d) than that caused by the $n \rightarrow n-1$ pathway because of the large mass difference between the parent and daughter ions. In the present condition, the daughter ions caused by $n \rightarrow n-3$ dissociations were reflected before the deceleration plate. Therefore, the energy focusing effect was ineffective in these daughter ions.

Figure 9 summarizes the size distribution of the daughter ions, $K^+(AN)_m$, formed by metastable dissociation from each parent ion, $K^+(AN)_n$, in the drift region. The metastable dissociation pathway of $n \rightarrow n-1$ (AN-loss) was observed for all parent sizes. In addition, only from the parent ions of n=6, 9, and 12, the pathway of $n \rightarrow n-3$ [$(AN)_3$-loss] was also observed. The pathway of $n \rightarrow n-2$ [$(AN)_2$-loss] was also weakly observed from n=5 and 8. No daughter ions from $K^+(AN)$ and $K^+(AN)_2$ were detected in the mass spectrum (not shown in Figs. 8 and 9).

B. Metastable dissociation of $K^+(AN)_n$ ions formed in the source by ion–molecule reactions

In order to compare the size-dependent pathways observed in metastable dissociation of $K^+(AN)_n$ photoions, we have also examined metastable dissociation in $K^+(AN)_n$ ions formed by ion–molecule reactions in the cluster source as shown in Fig. 10. Peaks denoted by circles were assigned to daughter ions caused by metastable dissociation in the first field-free drift region of reflectron TOF-MS. This mass spectrum was measured at a condition with U_k=+900 V and $U_0 \sim +1150$ V, in which most parent ions were not reflected back to the detector. Thus the ratio of the daughter ions to the parent ions was larger in Fig. 10 than in Fig. 2(b). However, due to relatively broad kinetic energy distribution of ions, the parent ions were also observed along with the daughter ions even with $U_k < U_0$. This is probably attributed to a long pulse width of cluster ions before acceleration. In other words, broad positional distribution of ions in the acceleration electrodes causes broad kinetic energy distribution of the accelerated ions. In this mass spectrum, the daughter ions caused by metastable dissociation pathway of the $n \rightarrow n-3$

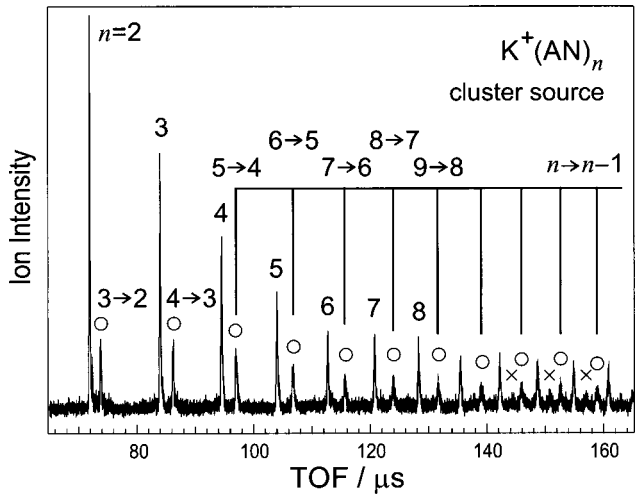

FIG. 10. The mass spectrum of $K^+(AN)_n$ ions produced by ion–molecule reaction in the cluster source. This spectra was measured at $U_k=+900$ V and $U_0\sim+1150$ V. The number in the figure represents n of parent $K^+(AN)_n$ ions. Peaks denoted by circles are assigned to daughter ions caused by metastable dissociation in the first field-free drift region of reflectron TOF-MS. Peaks denoted by × are assignable to $K^+(AN)_n(H_2O)$ ($n=10$–12) ions which arise from the presence of water impurity.

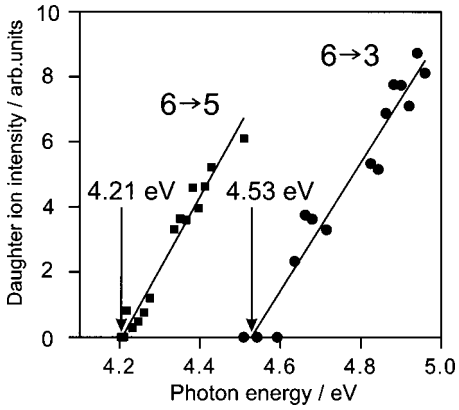

FIG. 11. Plots of daughter ion intensities caused by metastable dissociation of $K^+(AN)_6\rightarrow K^+(AN)_5+AN$ (6→5, ■) and $K^+(AN)_6\rightarrow K^+(AN)_3+(AN)_3$ (6→3, ●) as a function of the photon energy of the ionization laser.

were not observed, but those caused by $n\rightarrow n-1$ pathway for all the parent sizes. Namely, the $n\rightarrow n-3$ dissociation pathway was observed only in the metastable dissociation of $K^+(AN)_n$ caused by photoionization of *neutrals*.

As discussed in Sec. III A, the intracluster trimeric cyclization is initiated by the electron transfer from a K atom in *neutral* $K(AN)_n$ clusters. In the photoionization of these clusters, C–C bonds formed by the reactions in the neutral clusters are expected to be conserved, and dissociation reactions of the intramolecular bonds hardly proceed. Thus, structures of oligomers in the photoions are regarded to be similar to those of the neutral clusters. As a result, structural information of the *neutral* $K(AN)_n$ clusters is included in the fragmentation pattern of metastable dissociation of the *photoions*.

C. Geometrical structures and isomers of $K^+(AN)_n$ photoions

As discussed in the preceding section, the structures of photoions have a relation to the intracluster oligomerization in neutrals. The observed pathways with the loss of AN, $(AN)_2$, and $(AN)_3$ in metastable dissociation of $K^+(AN)_n$ photoions are assignable to elimination of AN molecule, linear dimeric oligomer and cyclic trimer (CHTCN), respectively. CHTCN and dimeric oligomer are formed by the intracluster oligomerization initiated by the electron transfer from a K atom in the neutrals. From $n=6$, 9, and 12, both pathways of AN and $(AN)_3$ loss were observed. In order to discuss structures of $K^+(AN)_6$ photoions, appearance energies of daughter ions were determined for the metastable dissociation of 6→5 and 6→3. Figure 11 shows plots of daughter ion intensities vs the photon energy of the ionization laser. From these plots, the appearance energies of daughter ions were determined to be 4.21 and 4.53 eV for 6→5 and 6→3, respectively. On the other hand, the I_{th} values of $K(AN)_6$ was determined to be 3.61 eV as shown in Table I. Because maximum excess energy in the photoion is equal to the difference between the photon energy and the I_{th}, dissociation energy is estimated from the difference of the appearance energy of the daughter ion and the I_{th} of the parent cluster. Therefore, the dissociation energy for the loss of $(AN)_3$ is determined to be 0.92 eV, which is larger than that for the loss of AN monomer, 0.60 eV. This reveals that the metastable dissociation reaction of $n\rightarrow n-1$ occurs preferentially in the parent cluster ions containing of both unreacted AN monomers and cyclic trimers (CHTCNs). Therefore, the observation of 6→3 pathway in $K^+(AN)_6$ indicates that the ion includes two CHTCNs. The two CHTCNs are formed by double trimeric cyclization reactions of six AN molecules and thus there are no unreacted AN molecules in $K(AN)_6$ clusters. In the same way, there is a possibility that k CHTCNs are formed by multiple cyclization reactions with $3k$ AN molecules in $K(AN)_n$ ($n=3k$; $k=3$ and 4). Such multiple cyclization has also been discussed in cationic oligomerization in styrene cluster cations.[17] By contrast, the observation of $n\rightarrow n-1$ pathway from $n=3k$ cluster ions indicates the existence of other structural isomers containing an AN molecule. In these isomers, one isomer contains unreacted $3k$ AN molecules, and others contain both CHTCN(s) and AN molecules. Although we have no idea on what isomer is most probable from the present results, this point will be discussed especially for $n=6$ in Sec. IV D by calculations based on statistical theory of unimolecular reaction. We have summarized these pathways of metastable dissociation in Fig. 12.

The $K^+(AN)_n$ ($n\geqslant 3$, $n\neq 6$, 9, and 12) cluster ions are expected to contain unreacted AN monomer(s), because the AN-loss was mainly observed in the fragmentation pattern of these cluster ions (Fig. 9). The $(AN)_2$-loss was weakly observed along with AN loss in the fragmentation pattern of $K^+(AN)_n$ ($n=5$ and 8). The $(AN)_2$ fragment is assignable to the linear dimeric oligomer. Although intensities of these daughter ions caused by $n\rightarrow n-2$ fragmentation pathway were too weak to determine the appearance energies, the AN-loss is expected to occur more preferentially than

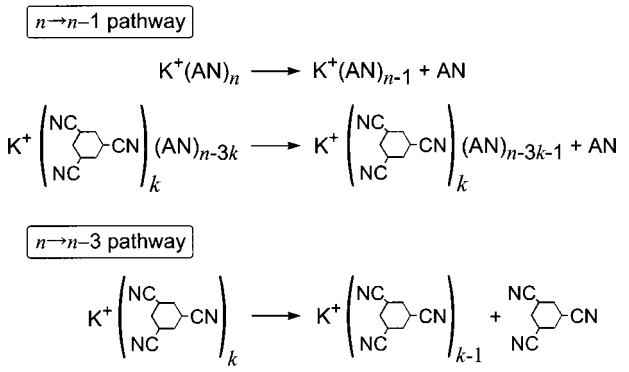

FIG. 12. Reaction schemes of metastable dissociation pathways of $n \rightarrow n-1$ and $n \rightarrow n-3$ from $K^+(AN)_n$ ($n=3k$; $k=2-4$) photoions.

$(AN)_2$-loss. Furthermore, the $(AN)_3$-loss is presumed to be less efficient than $(AN)_2$-loss. Therefore, in the same way as the discussion on $K^+(AN)_n$ ($n=3k$; $k=2-4$), there is an another isomer in which the dimeric oligomer and CHTCN(s) are contained for $n=5$ and 8. The result that $(AN)_2$-loss is hardly observed from $n=6$, 9, and 12 implies that the dimeric oligomer is not contained in $K^+(AN)_n$ ($n=6$, 9, and 12). This is explained by reactivity of dimeric oligomer and CHTCN. CHTCN shows high stability due to a cyclic structure, while there is a reactive radical site in the linear dimeric oligomer because it does not form the cyclic structure due to large ring strain. Owing to this activity of the dimer, the cyclic trimer is formed by a reaction between an AN monomer and the linear dimer in $n=6$, 9, and 12.

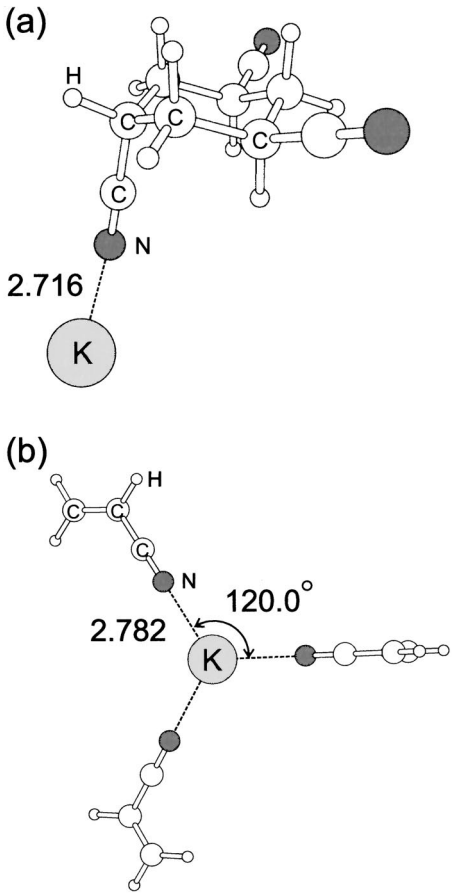

FIG. 13. Optimized structures of (a) K^+(CHTCN) (isomer 3^I) and (b) $K^+(AN)_3$ (isomer 3^{II}) calculated with B3LYP/6-31+G*. Bond lengths and angles are shown in Å and degrees, respectively.

D. Microcanonical rate constants based on the RRKM theory

In the discussion in Sec. III, it is concluded that there is a structural isomer for $K(AN)_3$ containing a CHTCN molecule as shown in Fig. 4. Thus the $K^+(AN)_3$ photoion has a corresponding isomer consisting of a K^+ ion and a CHTCN molecule (hereafter designated as isomer 3^I). However, the metastable dissociation of $3 \rightarrow 0$ expected from this isomer 3^I was not observed whereas only that of $3 \rightarrow 2$ pathway was observed, which proceeds from another isomer of K^+ and unreacted AN molecules (isomer 3^{II}), in the present experiment (Figs. 8 and 9). Because energies deposited in the photoions exceeds the dissociation energies for both of these isomers, the above observation should be explained by kinetics of these decay pathways rather than by energetics. For this purpose, we have calculated rate constants $k_{diss}(E)$ for the pathways of $3^I \rightarrow 0$ and $3^{II} \rightarrow 2$ as a function of the internal energy E, based on the restricted Rice–Ramsperger–Kassel–Marcus (RRKM) theory.[54]

In this theory, statistical RRKM calculations are carried out for the limited phase space of intermolecular modes. This treatment is based on the assumption that vibrational redistribution within a cluster from initially excited modes to intermolecular modes is much faster than dissociation process. In case of van der Waals cluster ions of polyatomic molecules such as benzene, the restricted RRKM model was proven to explain experimental results quantitatively.[55] Microcanonical rate constants in the RRKM theory is written as[56]

$$k_{diss}(E) = \frac{\alpha}{h} \frac{N^{\sharp}(E-E_d)}{\rho(E)} \tag{3}$$

where E_d is the dissociation energy, α is the reaction path degeneracy, h is the Planck constant, $N^{\sharp}(E-E_d)$ is the sum of states in a transition state at energy $E-E_d$, and $\rho(E)$ is the density of states in the reactant cluster. The reduced phase space of the intermolecular vibrations were used to evaluate $N^{\sharp}(E-E_d)$ and $\rho(E)$. For evaluation of these values, we calculated optimized structures and intermolecular vibrational frequencies of each isomer by density functional theory (B3LYP/6-31+G*). Obtained structures of these cluster ions are shown in Fig. 13. The dissociation energies for $3^I \rightarrow 0$ and $3^{II} \rightarrow 2$ pathways were estimated to be $E_d=0.92$ and 0.68 eV, respectively, accounting for the zero-point energy correction. The frequencies of the transition states were assumed to be identical with that of the reactant cluster ions. Intermolecular stretching vibration was considered as the reaction coordinate and omitted for calculations of $N^{\sharp}(E-E_d)$. $N^{\sharp}(E-E_d)$ and $\rho(E)$ were calculated using a Whitten–Rabinovitch approximation.[57] The reaction path degeneracies were chosen as $\alpha=1$ and 3 for $3^I \rightarrow 0$ and $3^{II} \rightarrow 2$ pathways, respectively. Figure 14(a) shows the $k_{diss}(E)$

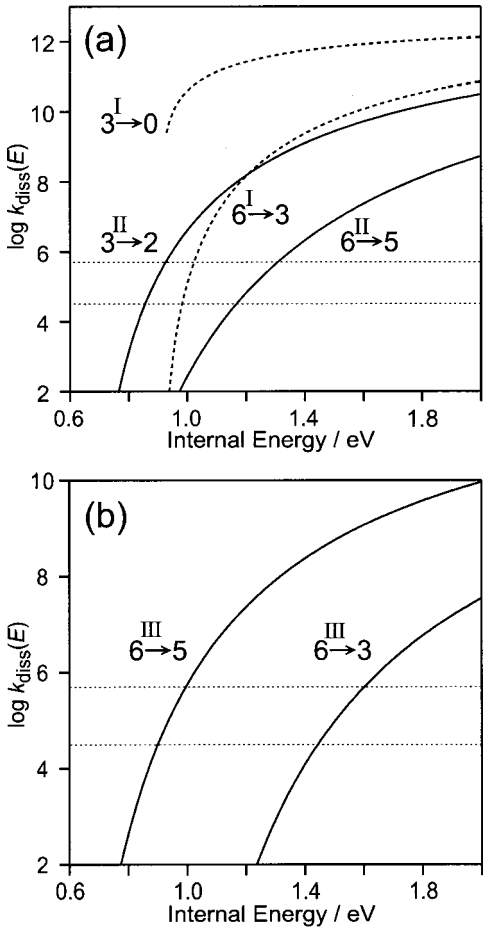

FIG. 14. Curves of microcanonical rate constants $k_{diss}(E)$ calculated by the restricted RRKM theory. (a) $K^+(CHTCN)\rightarrow K^+ + CHTCN$ ($3^I\rightarrow0$), $K^+(AN)_3\rightarrow K^+(AN)_2+AN$ ($3^{II}\rightarrow2$), $K^+(CHTCN)_2\rightarrow K^+(CHTCN)+CHTCN$ ($6^I\rightarrow3$), and $K^+(AN)_6\rightarrow K^+(AN)_5+AN$ ($6^{II}\rightarrow5$). (b) $K^+(CHTCN)(AN)_3\rightarrow K^+(CHTCN)(AN)_2+AN$ ($6^{III}\rightarrow5$) and $K^+(CHTCN)(AN)_3\rightarrow K^+(AN)_3+CHTCN$ ($6^{III}\rightarrow3$).

curves calculated by the restricted RRKM theory. Two dotted horizontal lines indicate the range of rate constants that lead to a metastable dissociation in the first field-free drift region in the present reflectron TOF-MS setup. In other words, this range corresponds to a time window of the present experiment. Although this time window is slightly shifted towards lower rates with increasing mass of the parent cluster ion, it can be approximated to be constant for all parent ions in the logarithmic scale. Obtained dissociation rates $k_{diss}(E)$ were found to increase abruptly with increasing internal energies. From a $k_{diss}(E)$ curve of $3^{II}\rightarrow2$ pathway, metastable dissociation from the isomer 3^{II} with an internal energy of ~0.9 eV was found to be observed in the present setup. By contrast, in the $3^I\rightarrow0$ pathway, fast dissociation process ($k_{diss}>10^9$ s^{-1}) was found to proceed when the internal energy of the isomer 3^I is larger than E_d (0.92 eV), and thus this process cannot be observed in the present time window. This behavior is explained by small number of intermolecular vibrational degrees of freedom of the isomer 3^I in comparison with that of the isomer 3^{II}. Therefore, missing of the $3\rightarrow0$ pathway is related to metastable dissociation dynamics and does not indicate the absence of isomer 3^I, $K^+(CHTCN)$, in $n=3$ clusters.

For the metastable dissociation of $6\rightarrow3$ and $6\rightarrow5$ pathways, we also calculated $k_{diss}(E)$ curves by the restricted RRKM theory. First we considered the following two isomers; one consists of a K^+ ion and two CHTCN molecules (denoted as isomer 6^I with analogy of $n=3$) and another contains a K^+ ion and six unreacted AN molecules (denoted as isomer 6^{II}). These isomers 6^I and 6^{II} are considered to be reactants in the $6\rightarrow3$ and $6\rightarrow5$ pathways, respectively. Intermolecular vibrational frequencies of these clusters were estimated from those obtained for $n=3$ in the above calculations. The reaction path degeneracies were $\alpha=2$ and 6 for the $6^I\rightarrow3$ and $6^{II}\rightarrow5$ pathways, respectively. Dissociation energies for these pathways were obtained from the appearance energies of daughter ions (Fig. 11) and the I_{th} of $K(AN)_6$ (Table I). Calculated $k_{diss}(E)$ curves [Fig. 14(a)] shows that daughter ions can be observed in present time window in both pathways. For $n=6$ cluster ions, another isomer can be considered which is described by $K^+(CHTCN)(AN)_3$, namely, consisting of a K^+ ion, one CHTCN, and unreacted three AN molecules (denoted as isomer 6^{III}). In order to specify a dissociation pathway from this isomer 6^{III}, $k_{diss}(E)$ curves for $6^{III}\rightarrow5$ and $6^{III}\rightarrow3$ pathways from this isomer were also calculated as shown in Fig. 14(b). Internal energy needed for the $6^{III}\rightarrow5$ pathway was found to be about 0.6 eV smaller than that for the $6^{III}\rightarrow3$ pathway in the present time window. A decay rate constant for $6^{III}\rightarrow5$ was found to be about three orders of magnitude larger than that for $6^{III}\rightarrow3$. Thus, the $6^{III}\rightarrow5$ pathway is considered to be dominant in dissociation from the isomer 6^{III}. From these considerations, it is confirmed that the $6\rightarrow3$ pathway relates to metastable dissociation of the isomer 6^I, $K^+(CHTCN)_2$, whereas both the isomers of 6^{II} and 6^{III} have a possibility to contribute the $6\rightarrow5$ pathway. In the analysis of metastable dissociation by using the statistical theory as shown above, it is clearly shown that several different isomers coexist for $n=3$ and 6 clusters, corresponding to the reaction products of propagation steps in intracluster oligomerization. Plural structural isomers are also expected to exist generally for other sizes of $K(AN)_n$ clusters.

V. CONCLUSION

In the present study, intracluster bond-formation (oligomerization) reactions initiated by electron transfer have been investigated by photoionization mass spectrometry of clusters of a K atom and AN molecules. In the photoionization mass spectrum of $K(AN)_n$, magic numbers were observed at $n=3k$ ($k=1$–4), as in the previous studies.[31,33] By comparison with the previous studies of $(AN)_n^-$ cluster anions,[21,25,28,30] these magic numbers are found to relate with the formation of a cyclohexane derivative (CHTCN) in intracluster trimeric cyclization initiated by electron transfer from a K atom in $K(AN)_n$. In addition, size-specific elimination reactions in $K(AN)_n$ were also observed; HCN elimination from $n\geqslant3$ clusters and H_2 elimination from $n=3$ and 6. Theoretical calculations showed that these elimination reactions are found to be induced by an excess energy generated in

CHTCN formation. This reaction mechanism is also consistent with the experimental result that no elimination reaction is observed from $n=2$.

Metastable dissociation of $K^+(AN)_n$ photoions was also examined in order to confirm the occurrence of the intracluster cyclization reaction. In the present experimental condition, an excess energy deposited in the photoions was relatively small, because the photoionization was a one-photon process. Therefore, sequential dissociation processes can hardly occur from a given parent ion. From an analysis of mass spectra of fragment ions (daughter ions), the dissociation pathway of $n \rightarrow n-1$ (AN-loss) was found for all parent ions. In addition, from the parent ions of $n=6$, 9, and 12, the pathway of $n \rightarrow n-3$ ($(AN)_3$-loss) was strongly observed. These size-dependent pathways are explained by CHTCN formation by oligomerization reaction in neutral $K(AN)_n$ clusters. From the measurements of appearance energies of daughter ions, the $n \rightarrow n-1$ pathway was found to be dominant for parent cluster ions containing unreacted AN molecules. By contrast, the observation of $n \rightarrow n-3$ pathways from $K^+(AN)_n$ ($n=3k$; $k=2-4$) reveals that k CHTCN molecules exist in the parent ions. These CHTCN molecules are formed by intracluster multiple trimeric cyclization reactions with $3k$ AN molecules in neutral clusters. Thus it is concluded that there are at least two types of structural isomers in the $n=3k$ clusters; one isomer contains at least one unreacted AN molecule, and another includes k CHTCN molecules. Kinetic effects in the observation of metastable dissociation was also examined by the restricted RRKM theory. From the estimation of microcanonical dissociation rate constants for $K^+(AN)_3$ parent ions, absence of $3 \rightarrow 0$ decay pathway in the present observation is explained by the kinetic effect; the rate constant of CHTCN-loss ($3 \rightarrow 0$ pathway) is found to be too high to detect the process in the present time window. In the calculation of rate constants from three possible $K^+(AN)_6$ parent ion structures, the $6 \rightarrow 3$ pathway is found to be attributed to the CHTCN dissociation from the $K^+(CHTCN)_2$ parent ions (isomer 6^{I}), whereas $K^+(AN)_6$ (isomer 6^{II}) and $K^+(CHTCN)(AN)_3$ (isomer 6^{III}) are both candidates of the parent ions for the $6 \rightarrow 5$ pathway. In conclusion, coexistence of the isomers corresponding to the sequential cyclization reaction products are clearly shown from the present observation of metastable dissociation and the calculation of decay rate constants by the RRKM theory.

ACKNOWLEDGMENTS

The authors wish to thank Mr. Keizo Tsukamoto for the construction of the experimental apparatus. The authors thank the Computer Center of the Institute for Molecular Science for provision of the Fujitsu VPP5000 computer. This work has been supported in part by a Grant-in-Aid for Scientific Research from the Japanese Ministry of Education, Science, Sports and Culture. Financial support from Mitsubishi Foundation is also acknowledged. One of the authors (K.O.) is supported by the Research Fellowship of the Japan Society for the Promotion of Science for Young Scientists.

[1] J. F. Garvey, W. R. Peifer, and M. T. Coolbaugh, Acc. Chem. Res. **24**, 48 (1991), and references therein.
[2] M. S. El-Shall and C. Marks, J. Phys. Chem. **95**, 4932 (1991).
[3] M. T. Coolbaugh, G. Vaidyanathan, W. R. Peifer, and J. F. Garvey, J. Phys. Chem. **95**, 8337 (1991).
[4] S. G. Whitney, M. T. Coolbaugh, G. Vaidyanathan, and J. F. Garvey, J. Phys. Chem. **95**, 9625 (1991).
[5] M. T. Coolbaugh and J. F. Garvey, Chem. Soc. Rev. **21**, 163 (1992).
[6] M. T. Coolbaugh, S. G. Whitney, G. Vaidyanathan, and J. F. Garvey, J. Phys. Chem. **96**, 9139 (1992).
[7] B. C. Guo and A. W. Castleman, Jr., J. Am. Chem. Soc. **114**, 6152 (1992).
[8] J. Wang, G. Javahery, S. Petrie, and D. K. Bohme, J. Am. Chem. Soc. **114**, 9665 (1992); J. Wang, G. Javahery, S. Petrie, A. C. Hopkinson, and D. K. Bohme, Angew. Chem. Int. Ed. Engl. **33**, 206 (1994).
[9] J. S. Brodbelt, C.-C. Liou, S. Maleknia, T.-Y. Lin, and R. J. Lagow, J. Am. Chem. Soc. **115**, 11069 (1993).
[10] G. M. Daly and M. S. El-Shall, J. Phys. Chem. **98**, 696 (1994).
[11] M. T. Coolbaugh, G. Vaidyanathan, and J. F. Garvey, Int. Rev. Phys. Chem. **13**, 1 (1994).
[12] G. M. Daly, Y. B. Pithawalla, Z. Yu, and M. S. El-Shall, Chem. Phys. Lett. **237**, 97 (1995).
[13] S. R. Desai, C. S. Feigerle, and J. C. Miller, J. Phys. Chem. **99**, 1786 (1995).
[14] M. S. El-Shall, G. M. Daly, Z. Yu, and M. Meot-Ner (Mautner), J. Am. Chem. Soc. **117**, 7744 (1995).
[15] M. Y. M. Lyktey, T. Rycroft, and J. F. Garvey, J. Phys. Chem. **100**, 6427 (1996).
[16] M. S. El-Shall and Z. Yu, J. Am. Chem. Soc. **118**, 13058 (1996).
[17] Y. B. Pithawalla, J. Gao, Z. Yu, and M. S. El-Shall, Macromolecules **29**, 8558 (1996).
[18] Q. Zhong, L. Poth, Z. Shi, J. V. Ford, and A. W. Castleman, Jr., J. Phys. Chem. B **101**, 4203 (1997).
[19] K. Hiraoka, T. Sugiyama, T. Kojima, J. Katsuragawa, and S. Yamabe, Chem. Phys. Lett. **349**, 313 (2001).
[20] Y. B. Pithawalla, M. Meot-Ner, J. Gao, M. S. El-Shall, V. I. Baranov, and D. K. Bohme, J. Phys. Chem. A **105**, 3908 (2001).
[21] T. Tsukuda and T. Kondow, J. Chem. Phys. **95**, 6989 (1991).
[22] T. Tsukuda and T. Kondow, Chem. Phys. Lett. **197**, 438 (1992).
[23] T. Tsukuda and T. Kondow, J. Phys. Chem. **96**, 5671 (1992).
[24] T. Tsukuda, A. Terasaki, T. Kondow, M. G. Scarton, C. E. Dessent, G. A. Bishea, and M. A. Johnson, Chem. Phys. Lett. **201**, 351 (1993).
[25] T. Tsukuda and T. Kondow, J. Am. Chem. Soc. **116**, 9555 (1994).
[26] Y. Fukuda, T. Tsukuda, A. Terasaki, and T. Kondow, Chem. Phys. Lett. **242**, 121 (1995).
[27] M. Ichihashi, T. Tsukuda, S. Nonose, and T. Kondow, J. Phys. Chem. **99**, 17354 (1995).
[28] Y. Fukuda, T. Tsukuda, A. Terasaki, and T. Kondow, Chem. Phys. Lett. **260**, 423 (1996).
[29] T. Tsukuda, T. Kondow, C. E. H. Dessent, C. G. Bailey, M. A. Johnson, J. H. Hendricks, S. A. Lyapustina, and K. H. Bowen, Chem. Phys. Lett. **269**, 17 (1997).
[30] Y. Fukuda, M. Ichihashi, A. Terasaki, T. Kondow, K. Osoda, and K. Narasaka, J. Phys. Chem. A **105**, 7180 (2001).
[31] K. Ohshimo, F. Misaizu, and K. Ohno, J. Phys. Chem. A **104**, 765 (2000).
[32] H. Tsunoyama, K. Ohshimo, F. Misaizu, and K. Ohno, J. Am. Chem. Soc. **123**, 683 (2001); J. Phys. Chem. A **105**, 9649 (2001); K. Ohshimo, A. Furuya, H. Tsunoyama, F. Misaizu, and K. Ohno, Int. J. Mass Spectrom. **216**, 29 (2002).
[33] K. Ohshimo, H. Tsunoyama, F. Misaizu, and K. Ohno, Eur. Phys. J. D **16**, 107 (2001).
[34] T. D. Märk and O. Echt, in *Clusters of Atoms and Molecules II*, edited by H. Haberland (Springer-Verlag, Berlin, 1994).
[35] P. P. Radi, T. L. Bunn, P. R. Kemper, M. E. Molchan, and M. T. Bowers, J. Chem. Phys. **88**, 2809 (1988).
[36] P. Scheier and T. D. Märk, Phys. Rev. Lett. **59**, 1813 (1987); Int. J. Mass Spectrom. Ion Processes **102**, 19 (1990).
[37] C. Bréchignac, Ph. Cahuzac, J. Leygnier, and J. Weiner, J. Chem. Phys. **909**, 1492 (1989); C. Bréchignac, Ph. Cahuzac, F. Carlier, M. de Frutos, and J. Leygnier, *ibid.* **93**, 7449 (1990); C. Bréchignac, H. Busch, Ph. Cahuzac, and J. Leygnier, *ibid.* **101**, 6992 (1994).
[38] L. Poth, Z. Shi, Q. Zhong, and A. W. Castleman, Jr., J. Phys. Chem. A **101**, 1099 (1997).
[39] N. J. Kim, H. Kang, G. Jeong, Y. S. Kim, K. T. Lee, and S. K. Kim, J. Chem. Phys. **115**, 7002 (2001).
[40] J.-M. L'Hermite, F. Rabilloud, P. Labastie, and F. Spiegelman, Eur. Phys. J. D **16**, 77 (2001).

[41] C. P. Schulz, R. Haugstätter, H. U. Tittes, and I. V. Hertel, Z. Phys. D: At., Mol. Clusters **10**, 279 (1988).
[42] F. Misaizu, M. Sanekata, K. Tsukamoto, and K. Fuke, J. Phys. Chem. **96**, 8259 (1992).
[43] $K^+(AN)_n$−HCN or $K^+(AN)_n$−H_2 denote the ions caused by photoionization of neutral clusters produced by HCN or H_2 elimination reaction from $K(AN)_n$.
[44] J. Guo, T. Carrington, and S. V. Filseth, J. Chem. Phys. **115**, 8411 (2001).
[45] M. J. Frisch, G. W. Trucks, H. B. Schlegel *et al.*, GAUSSIAN 94, Revision E.2, Gaussian, Inc., Pittsburgh, PA, 1995.
[46] M. Khlifi, M. Nollet, P. Paillous, P. Bruston, F. Raulin, Y. Bénilan, and R. K. Khanna, J. Mol. Spectrosc. **194**, 206 (1999).
[47] H. Kühlewind, A. Kiermeier, and H. J. Neusser, J. Chem. Phys. **85**, 4427 (1986).
[48] S. Wei, Z. Shi, and A. W. Castleman, Jr., J. Chem. Phys. **94**, 8604 (1991).
[49] W. Kamke, B. Kamke, H. U. Kiefl, and I. V. Hertel, J. Chem. Phys. **84**, 1325 (1986).
[50] H. Shinohara, H. Sato, F. Misaizu, K. Ohashi, and N. Nishi, Z. Phys. D: At., Mol. Clusters **20**, 197 (1991).
[51] A. Kiermeier, B. Ernstberger, H. J. Neusser, and E. W. Schlag, J. Phys. Chem. **92**, 3785 (1988).
[52] C. P. Schulz, J. Hühndorf, P. Brockhaus, and I. V. Hertel, Z. Phys. D: At., Mol. Clusters **40**, 78 (1997).
[53] C. E. Moore, *Atomic Energy Levels, United States Department of Commerce* (National Bureau of Standards, Washington, D.C., 1949), Vol. I.
[54] D. F. Kelley and E. R. Bernstein, J. Phys. Chem. **90**, 5164 (1986).
[55] B. Ernstberger, H. Krause, A. Kiermeier, and H. J. Neusser, J. Chem. Phys. **92**, 5285 (1990); K. Ohashi and N. Nishi, *ibid.* **109**, 3971 (1998).
[56] P. J. Robinson and K. A. Holbrook, *Unimolecular Reactions* (Wiley-Interscience, London, 1972), p. 64; W. Forst, *Theory of Unimolecular Reactions* (Academic, New York, 1973), p. 68.
[57] G. Z. Whitten and B. S. Rabinovitch, J. Chem. Phys. **38**, 2466 (1963); P. J. Robinson and K. A. Holbrook, *Unimolecular Reactions* (Wiley-Interscience, London, 1972), p. 131.